ECOLE POLYTECHNIQUE FEDERALE DE LAUSANNE

SGM - 6th & 8th Semester, Fall 2024

CAVITATION AND INTERFACE PHENOMENA

Chapter 5: Vortex Cavitation

5.3: Flow Control for Tip Vortex Cavitation Mitigation

By Dr Ali Amini

Dr Mohamed FARHAT   Assistants: A. Sache, Th. Berger

EPFL – Cavitation Research Group, Avenue de Cour 33 bis, 1007 Lausanne

Tip vortex cavitation consequences

- **TVC** may occur in **axial** hydraulic machines
  - Risk of severe erosion in stationary and rotating parts

Visualization of TVC in an axial turbine

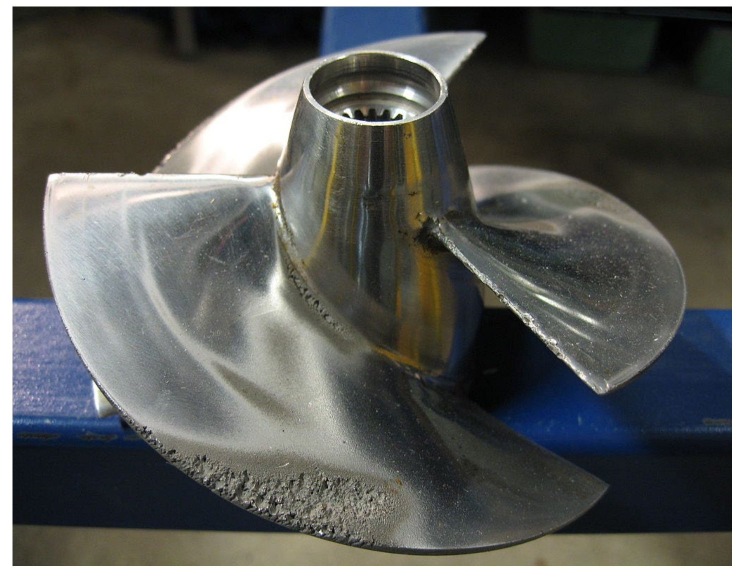

Erosion of the blade tip in a propeller

TVC Mitigation techniques

- Passive or active injections
  - Water or viscoelastic polymer solutions
- Adding artificial roughness to the tip
- Bulbous tips
- …

Suppressing Tip Vortex Cavitation by Winglets

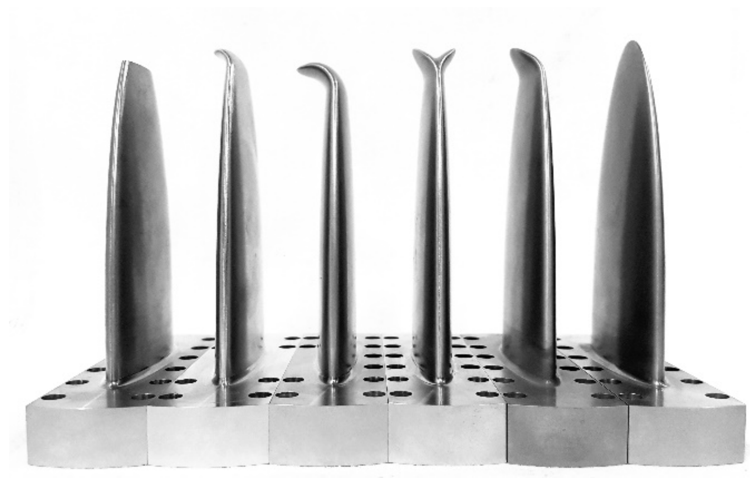

Ali Amini, Martino Reclari, Takeshi Sano, Masamichi Iino, and Mohamed Farhat. "Suppressing tip vortex cavitation by winglets." *Experiments in Fluids* 60, no. 11 (2019): 159.

Introduction

Tip vortices are a source of concern in aeronautics

➢ Lift-induced drag & flight hazards

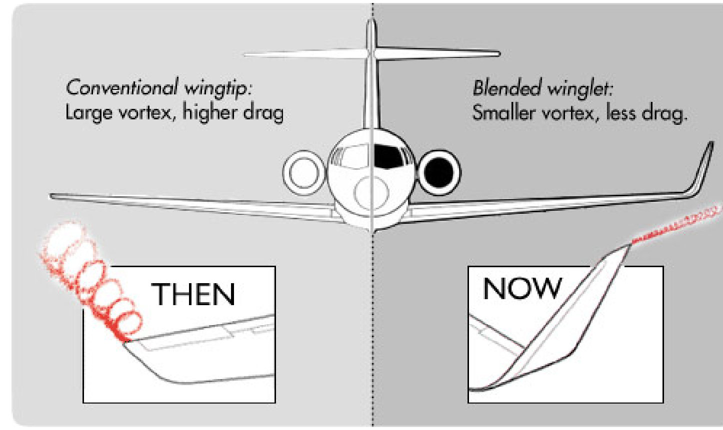

✓A common remedy is appending winglets to wingtips

- Widely used in commercial airplanes
- A large variety of winglets design
- No unique solution exists
- Each winglet has to be carefully designed based on the objectives and constraints.

Introduction

source: www.andritz.com

Anti-cavitation lips already exist, but …

- A survey on **44** projects performed at **LMH** during the last **15 years** revealed that

➢ Only **27%** → All on the **suction side**

- Usually have simple geometries

✓ A step towards **real winglet designs**

➢ Simple and generic geometries

➢ Physical aspects of the flow

Experimental Setup

The winglets are realized by **non-planar extensions** of the **original** section at various angles

- Design variables: θ & L_{BS}
- Smooth transition of the geometry

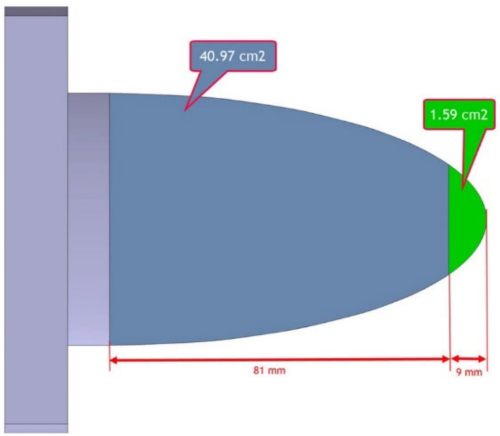

The affected area is max. 3.7% of the whole lifting surface.

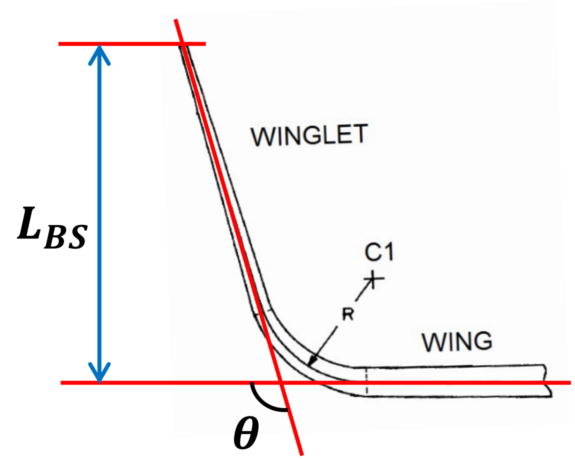

Dihedral angle: $\theta = 0°, \pm 45, \pm 90°$

Bent section length: $L_{BS} = 0.05S$ & $0.1S$

S: span of the baseline hydrofoil (90 mm)

Experimental Setup

Manufactured hydrofoils from bronze

***Upward &
Downward winglets***

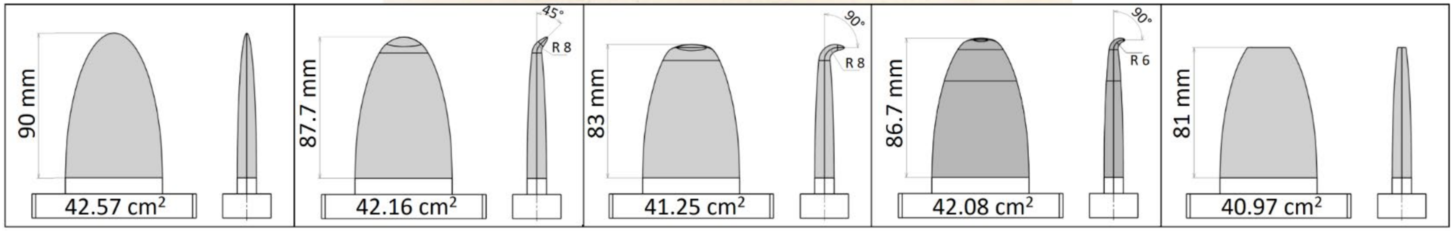

TVC inception results

Tests performed at $U_\infty = 15\ m/s$ and fully saturated water for **10%-bent winglets**.

- The **90° winglet bent toward the pressure side** shows an outstanding performance.

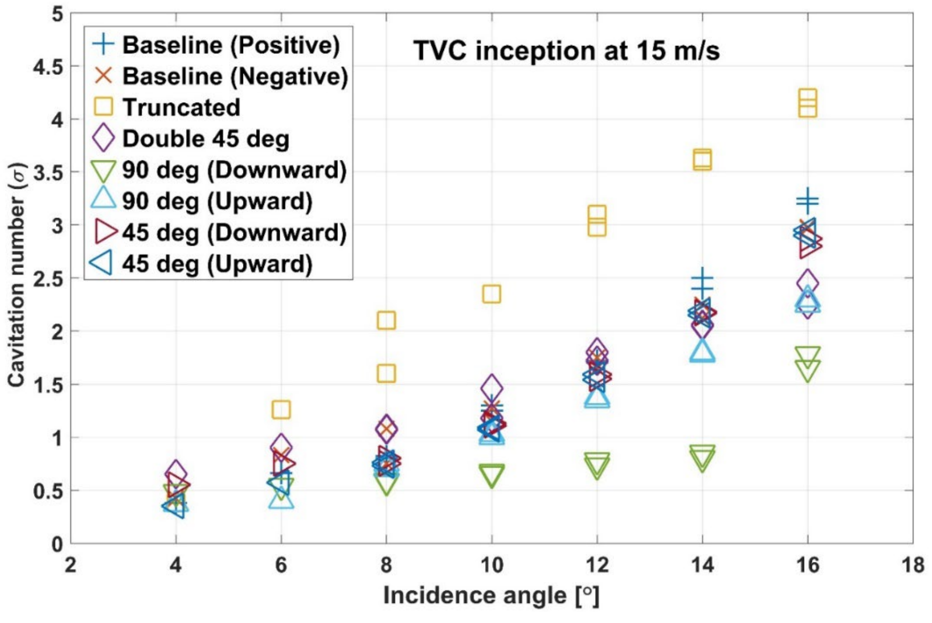

TVC inception results

Tests performed at $U_\infty = 15$ **m/s** and fully saturated water for **10%-bent winglets**.

- The **5%-bent** winglets are **less effective** in TVC mitigation.

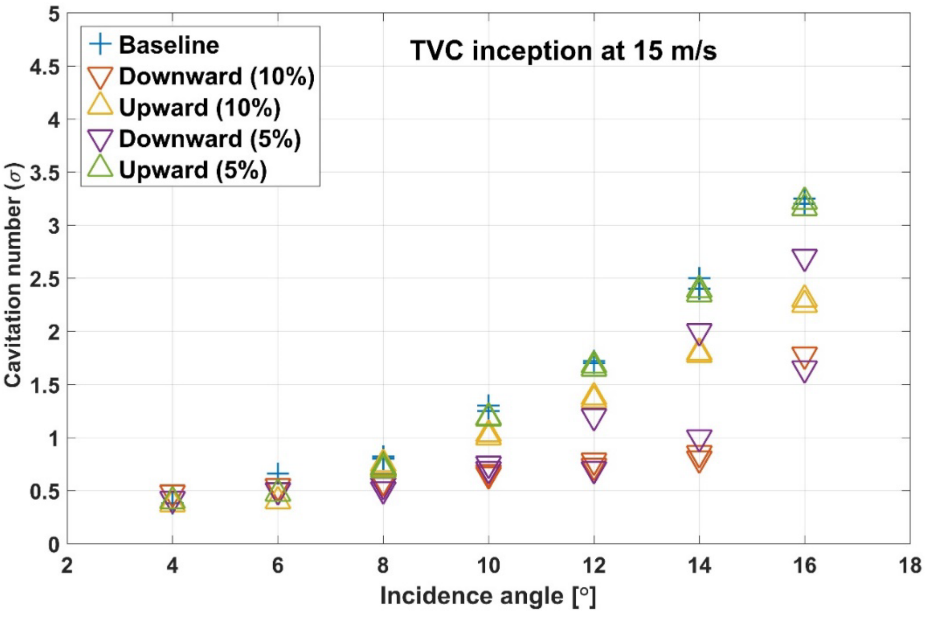

Flow visualizations

Effect of various winglets on TVC ($Re = 600{,}000$)

Test conditions: $\mathbf{U_\infty = 10\ m/s}$, $\boldsymbol{\alpha = 12°}$, $\boldsymbol{\sigma = 1.2}$

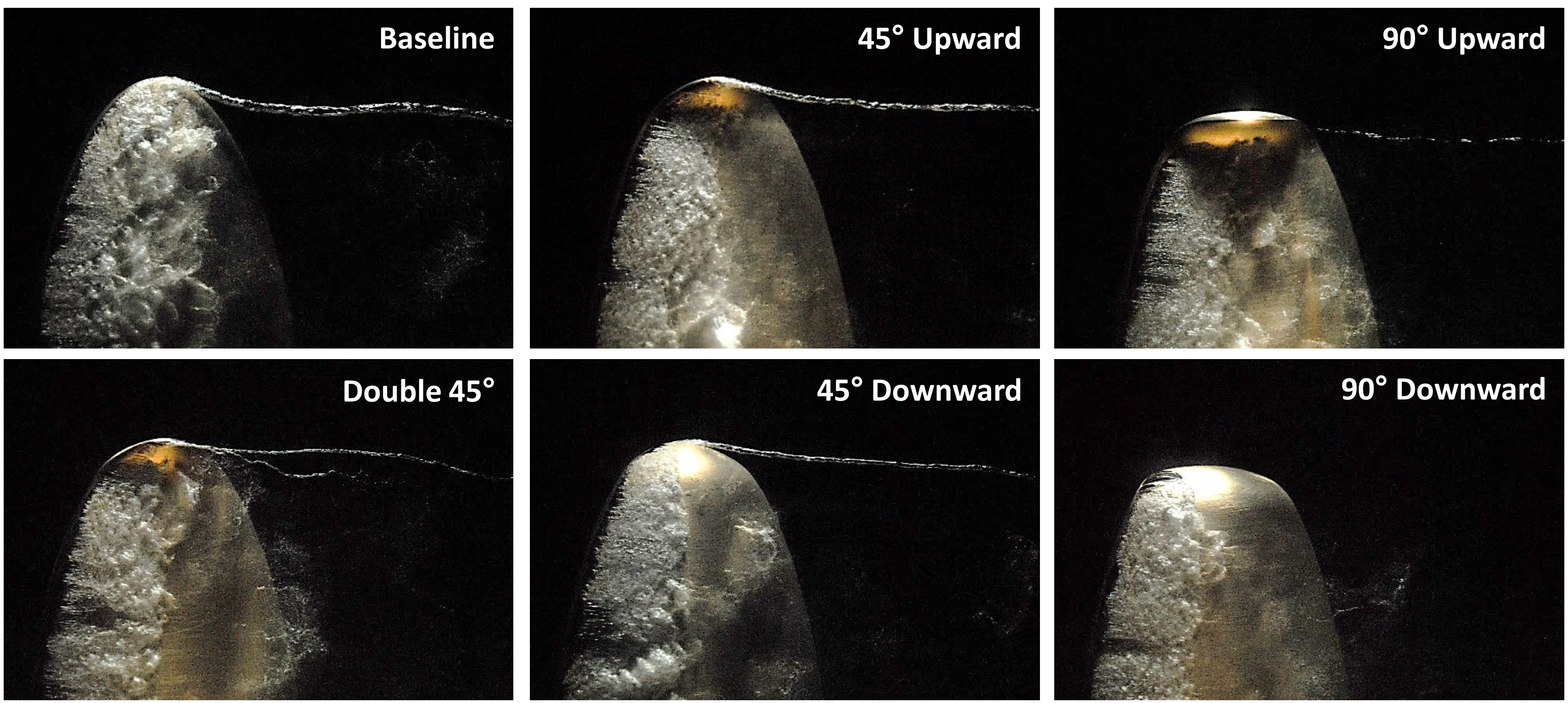

Flow visualizations

Effect of various winglets on TVC ($Re = 900{,}000$)

Test conditions: $U_\infty = 15\ \mathrm{m/s}$, $\alpha = 12°$, $\sigma = 1.2$

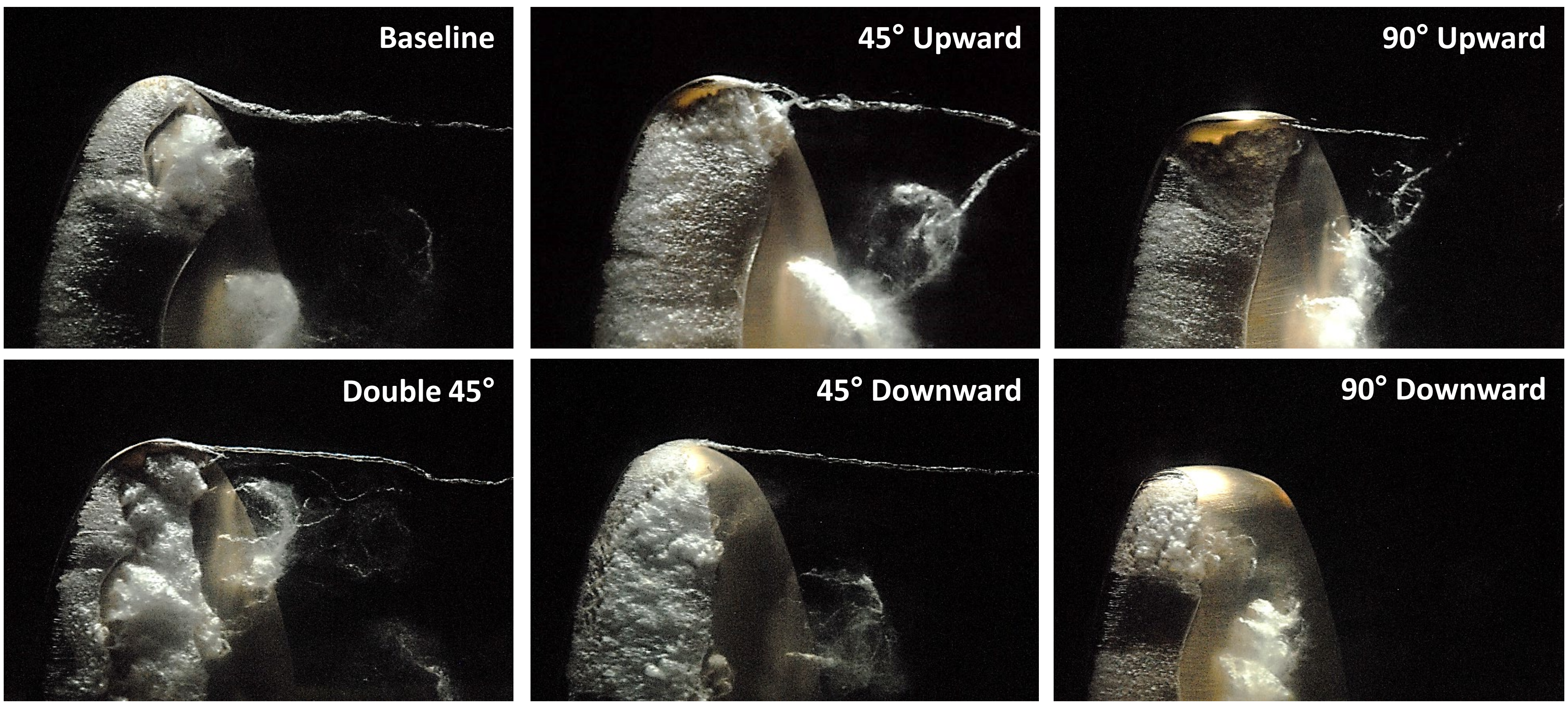

Lift & drag measurements

Measurements performed at 10 m/s to avoid cavitation

- Almost **similar** hydrodynamic performances are obtained for all the hydrofoils

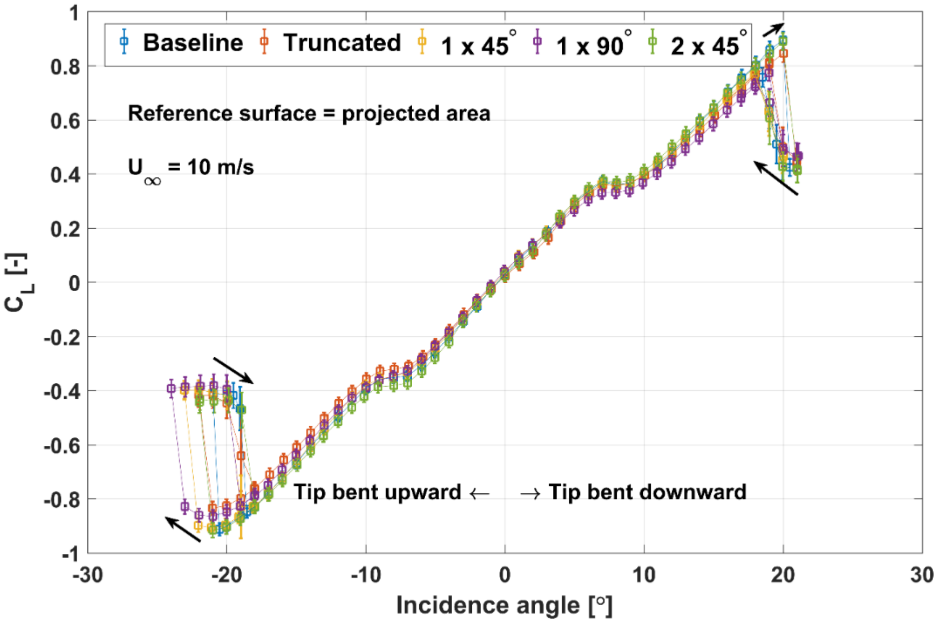

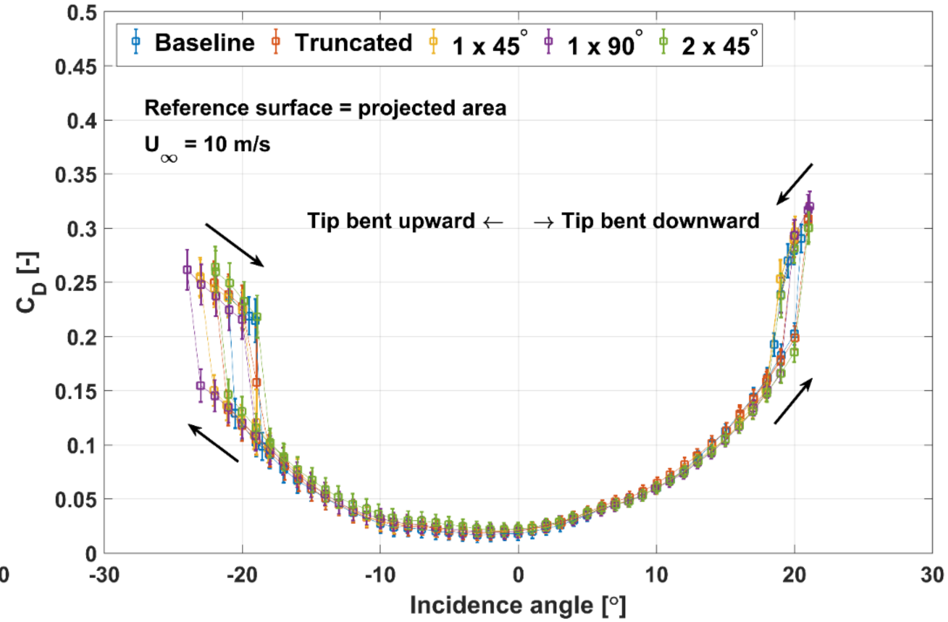

Stereo-PIV setup

- Double-pulsed laser (135 mJ/pulse)
- Seeding particles
  - Hollow glass spheres
  - Average diameter of 10 µm
- 1000 image-pairs for each flow condition
- Vector-to-vector resolution of 0.35 mm
- Wandering motion correction
  - Center detection by Graftieaux algorithm
  - 2D cubic spline interpolation
- Vatistas vortex model curve-fit

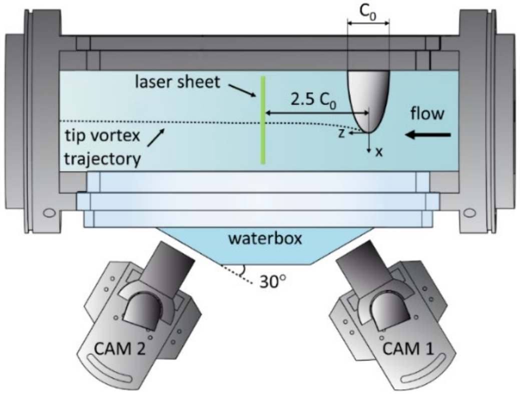

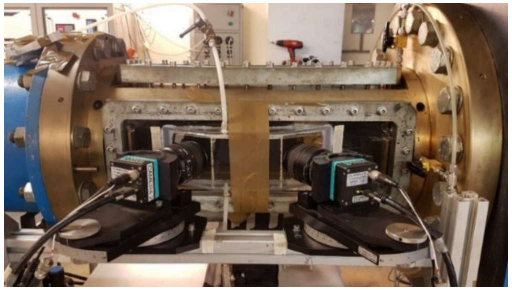

Velocimetry Results

Wandering effect and its correction

- Flow conditions: $U_\infty = \mathbf{10\ m/s}, \boldsymbol{\alpha} = \mathbf{12}°$
- 30 - 40% of variations between different hydrofoils
- Higher for downward configurations
- Sub-grid fluctuations

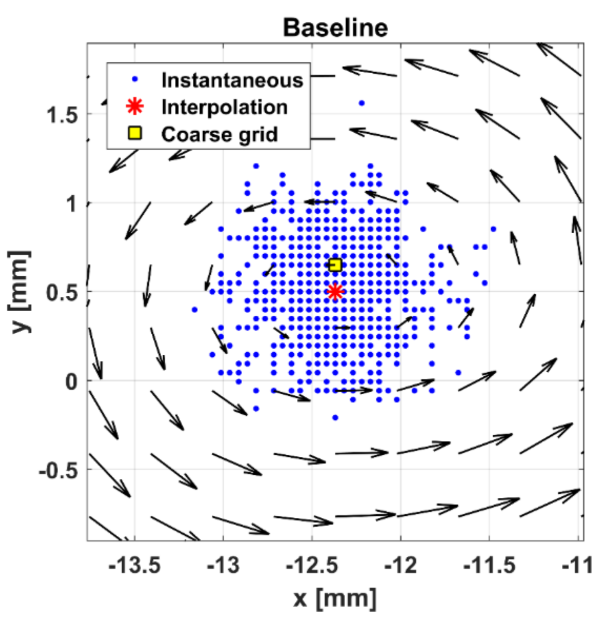

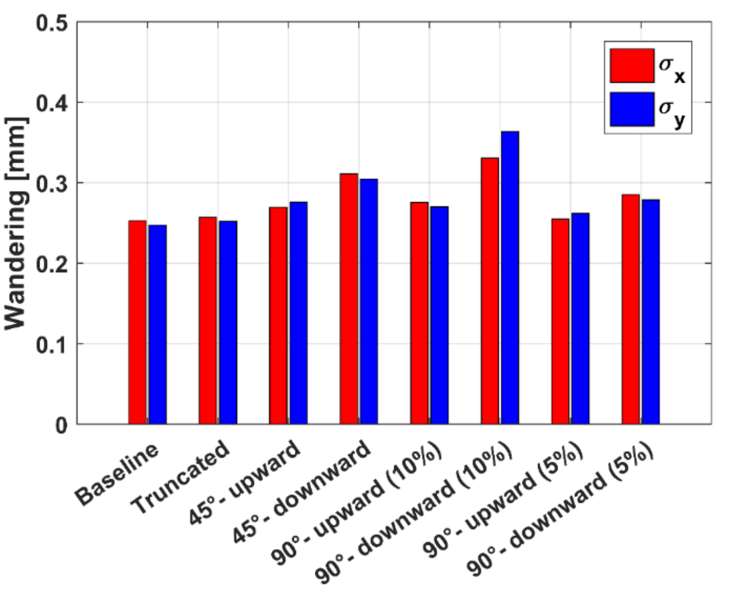

Stereo-PIV results

Contours of the **tangential** velocity

- Flow conditions: $\boldsymbol{U_\infty = 10\ \mathrm{m/s}, \alpha = 12^\circ}$

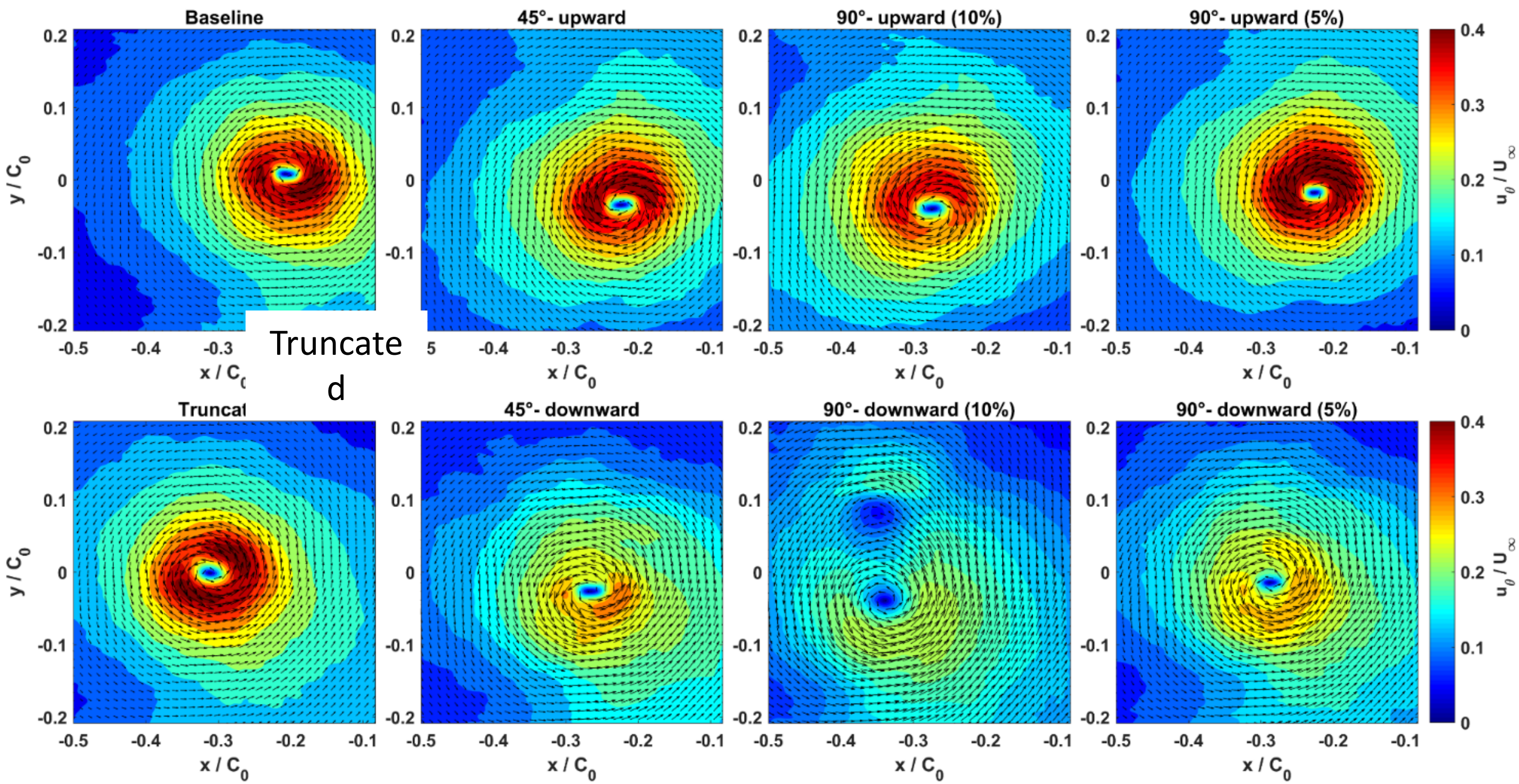

Velocimetry Results

Comparison of the tangential velocity profiles:

- Flow conditions: $\boldsymbol{U_\infty = 10\ \mathrm{m/s}\,, \alpha = 12°}$

- **90°-downward (10%)**
  - Outstanding suppression effects
  - Increasing the viscous radius ($\boldsymbol{r_c}$) by 70 %
  - Decreasing $\boldsymbol{v_{\theta_{max}}}$ to almost 50 %

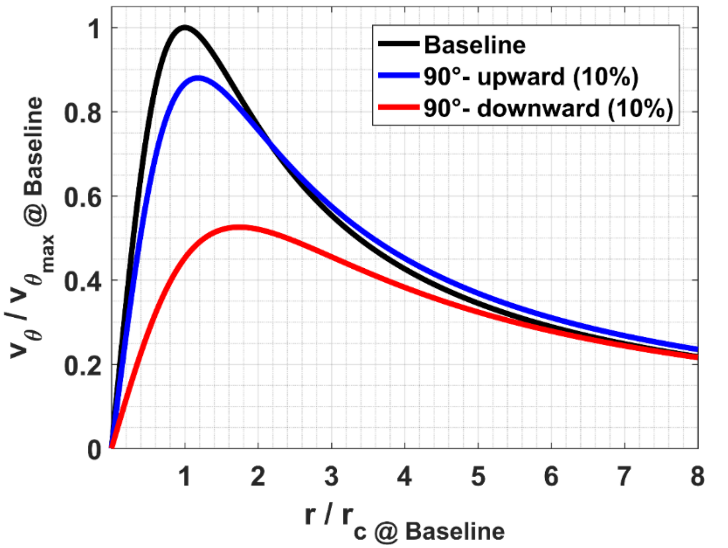

✓ $\boldsymbol{\Gamma}$ remains constant while $\boldsymbol{r_c}$ increases

✓ ***Viscous core thickening*** is the dominant mechanism of TVC mitigation

Velocimetry Results

Comparison of the tangential velocity profiles

- Same flow conditions: $U_\infty = 10\ \text{m/s}, \alpha = 12°$
- Azimuthally-averaged profiles

➢ Γ remains constant while r_c increases

➢ ***Viscous core thickening*** is the dominant mechanism of TVC mitigation

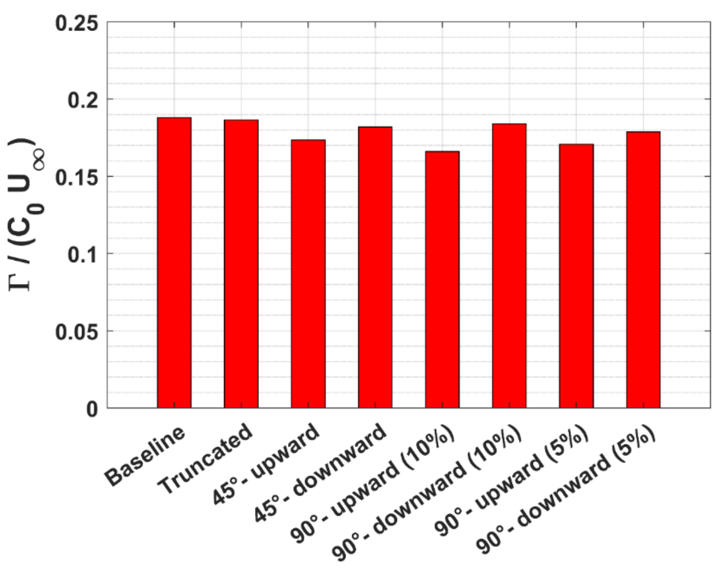

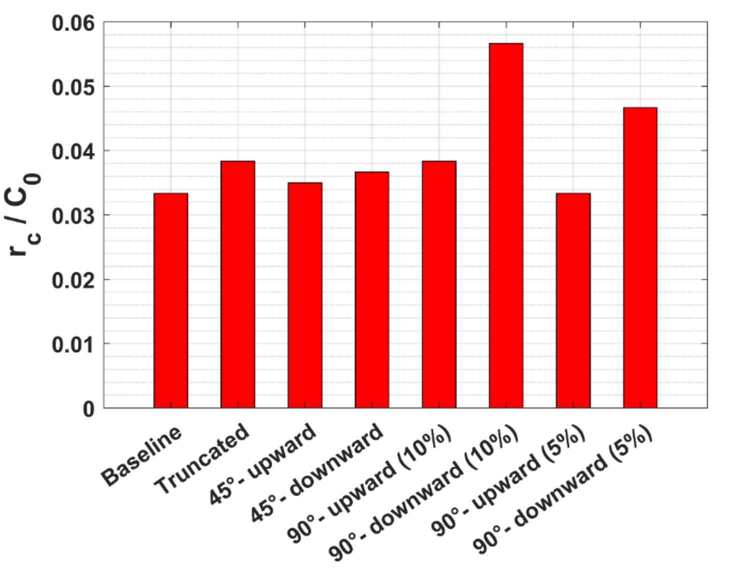

Velocimetry Results

Contours of the **axial** velocity

- Flow conditions: $\boldsymbol{U_\infty = 10\ \mathrm{m/s}, \alpha = 12°}$

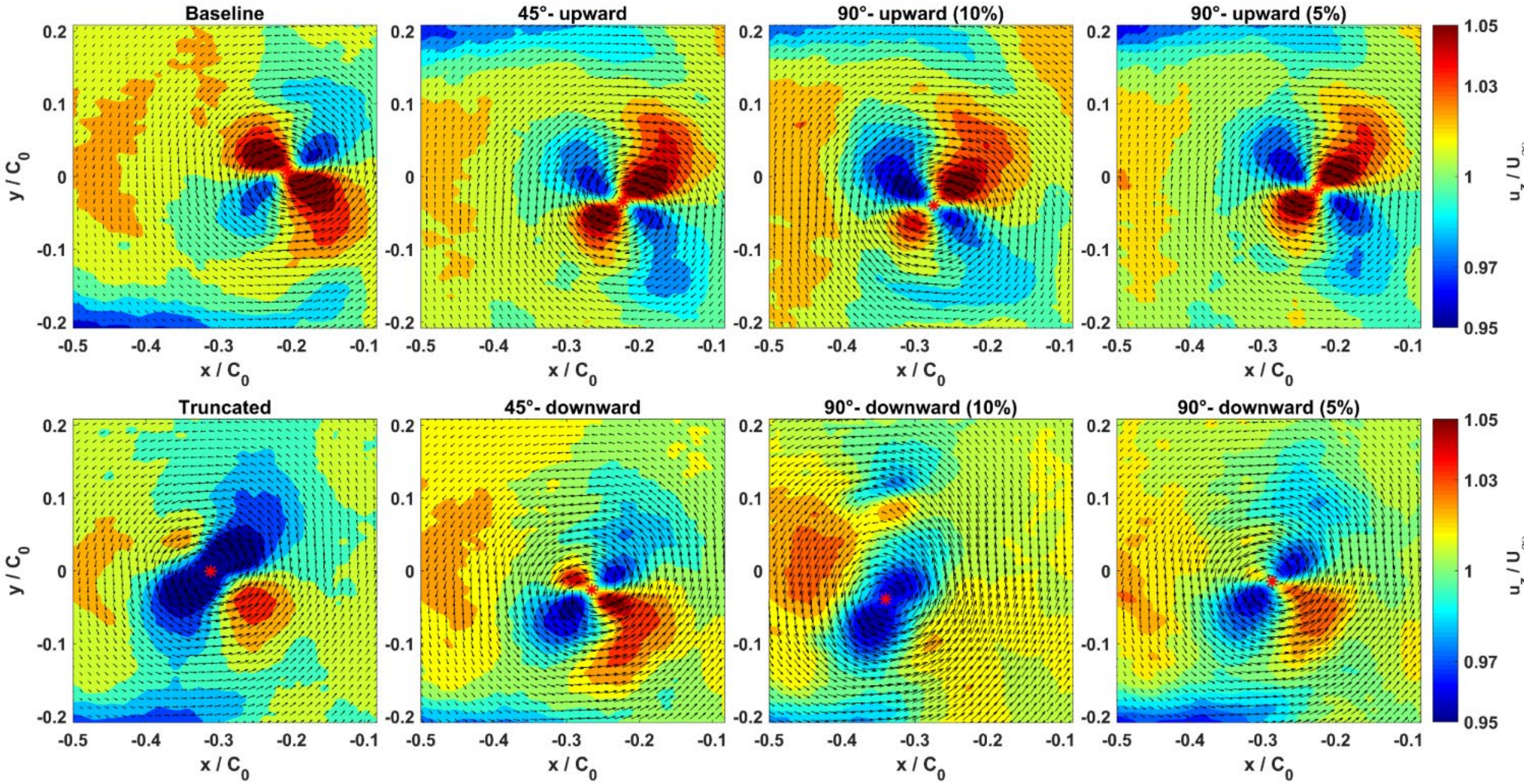

Velocimetry Results: Discussion

The higher effectiveness of the downward configurations is due to the fact that:

1) A downward-facing winglet facilitates the entrainment of the **wake** into the vortex flow,
2) which, in turn, increases the momentum diffusion rates, and thereby,
3) smooths down the velocity profiles.

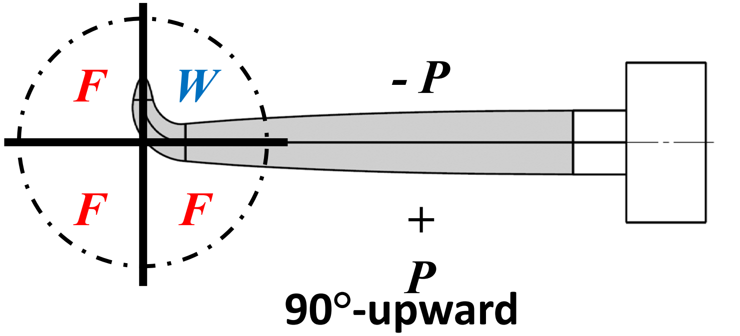

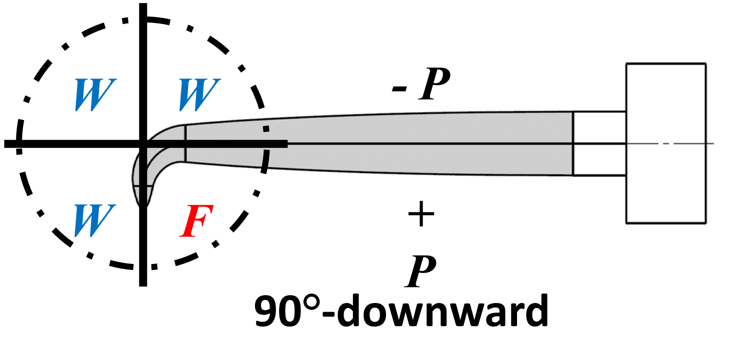

Velocimetry Results

Effect of incidence angle on Γ and r_c

- Flow conditions: $\boldsymbol{U_\infty = 10\ \mathrm{m/s}}$
- Similar trends are conserved

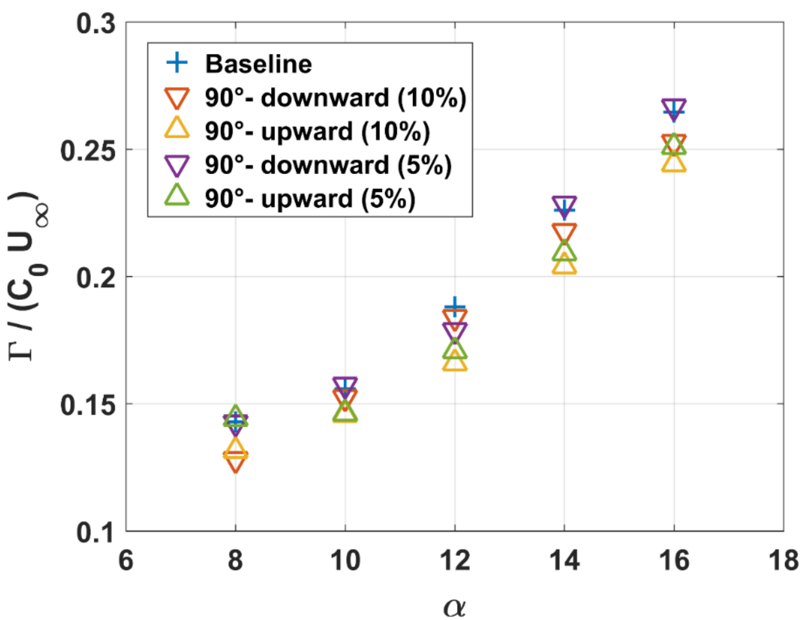

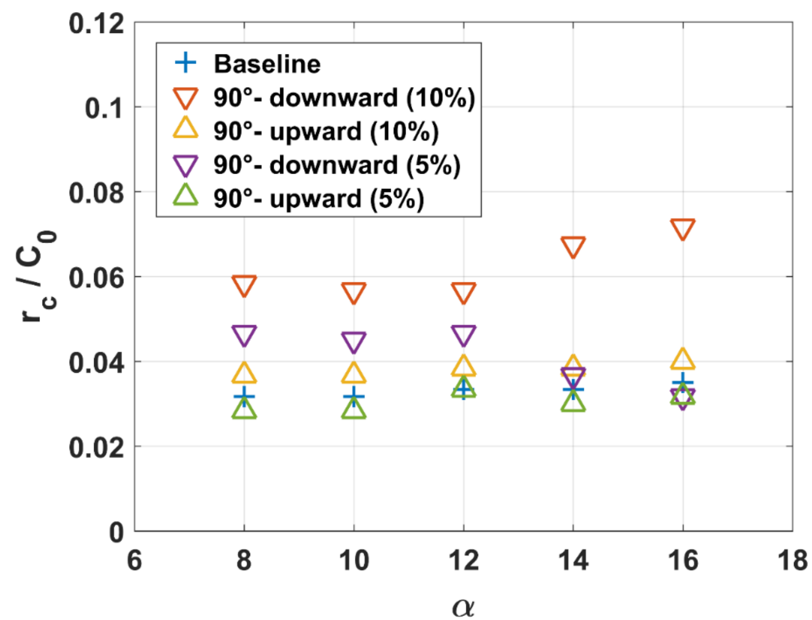

Conclusion

Effectiveness of nonplanar winglets in TVC suppression is investigated:

- Almost for all the flow conditions, the winglet-equipped hydrofoils perform better than the baseline hydrofoil in terms of delaying TVC.
- The hydrodynamic performances of the hydrofoils are **not** degraded by the winglets.
- For $\boldsymbol{L_{BS} = 0.1S}$, $\boldsymbol{\theta = 90}$° yielded much better results compared to $\boldsymbol{\theta = 45}$°.
- The negative dihedral angles (**downward**) are superior to the positive ones (**upward**), due to enhanced **wake entrainment** effects.
- Longer vertical sections outperform the shorter ones.
- Best configuration performance: **10%-bent 90°-downward**
  - ➢ Outstanding suppression (68% delay in inception)
  - ➢ Increasing the viscous core radius by 70%
  - ➢ Decreasing $\boldsymbol{v_{\theta_{max}}}$ to almost 50%

Mitigating Tip Vortex Cavitation by a Flexible Trailing Thread

Ali Amini, Jeonghwa Seo, Shin Hyung Rhee, and Mohamed Farhat. "Mitigating tip vortex cavitation by a flexible trailing thread." *Physics of Fluids* 31, no. 12 (2019): 127103.

TVC Suppression Mechanisms

Interaction of a flexible trailing thread with the cavitating vortex flow

- Flow conditions: $\alpha = 15°$, $U_\infty = 15$ m/s, and $\sigma = 1.8$
- Effect of the thread length ($\boldsymbol{L_t}$) on TVC suppression (thread diameter: $d_t = 0.7$ mm)
- C_0 is the root chord length of the hydrofoil ($C_0 = 60\ mm$)

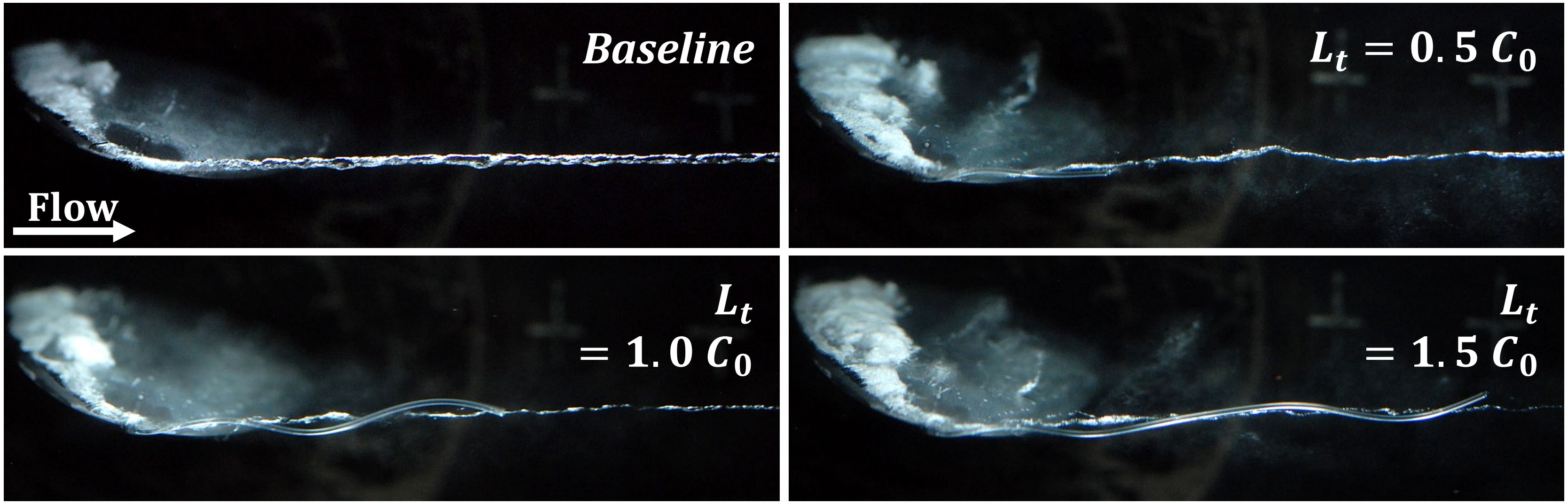

Analysis of the thread motion

- The most rigid thread tested under the following conditions → **Two stable** states
  - Test conditions: $\alpha = 10°$, $U_\infty = 10$ m/s, $\sigma = 1.2$, $d_t = 0.7$ mm and $L_t = 0.5\ C_0$

- Freestream velocity → Acceleration vs Deceleration → Static vs Dynamic response

- The thread should be flexible enough to align with the vortex and interact with it dynamically.

But, what does *flexible enough* mean?

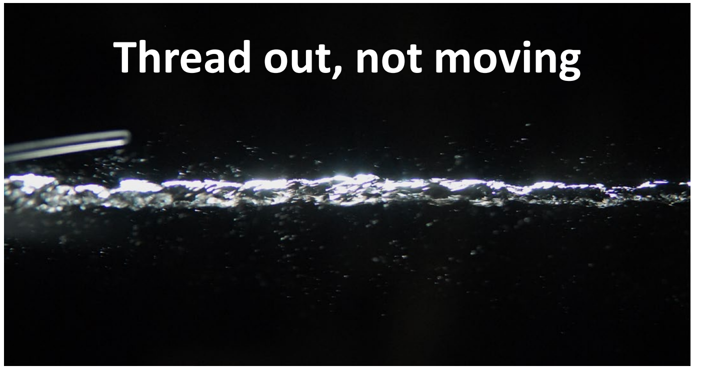

Analysis of the thread motion

The lateral motion of a flexible beam retained straight in axial flow is analyzed.

de Langre et al. (2007)

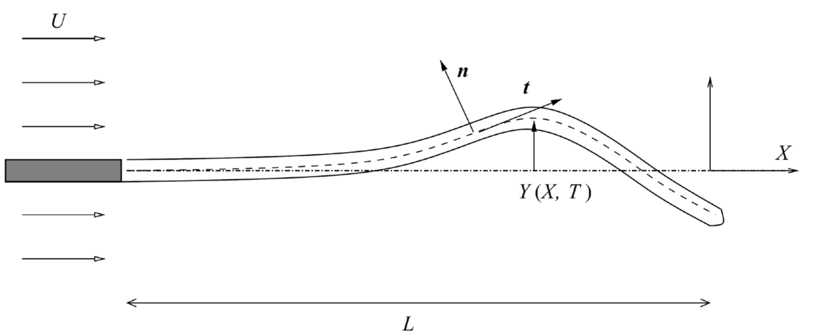

Non-dimensional velocity

$$u = \left(\frac{\rho A}{EI}\right)^{1/2} U_\infty L_t$$

flexural rigidity

fluid-induced forces

$$EI\frac{\partial^4 y}{\partial x^4} - \frac{\partial}{\partial x}\left(\Theta(x)\frac{\partial y}{\partial x}\right) + m\frac{\partial^2 y}{\partial t^2} = F_{fluid}$$

variation of local axial tension

Acceleration term
m: mass per unit length

TVC Suppression Mechanisms

- **Analysis of the thread motion**
  - Test conditions: $d_t = 0.5$ mm, $L_t = 1.5\ C_0$, $\alpha = 10°$ and $U_\infty = 10$ m/s
- **Harmonic waves** are travelling along the thread.
- The thread clearly encloses the vortex axis by **rotating** around it.

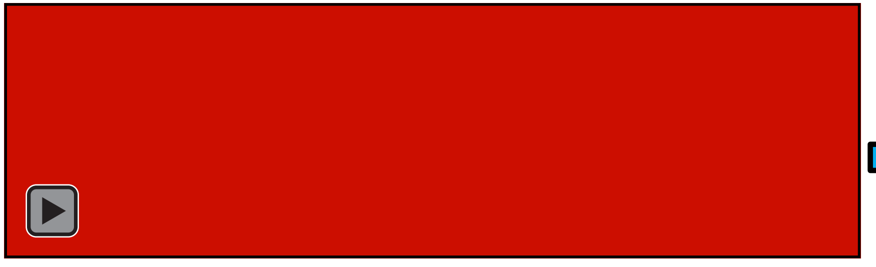

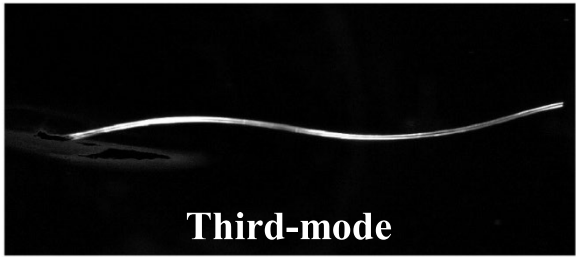

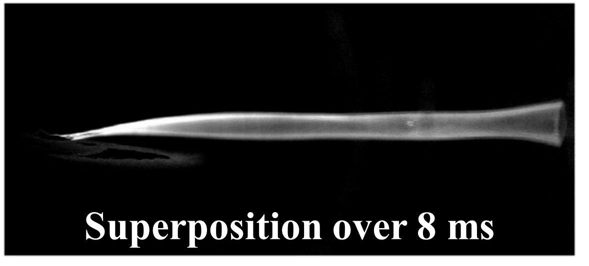

TVC Suppression Mechanisms

Dynamic interaction of the trailing thread and the vortex flow

- Flow conditions: $\boldsymbol{\alpha = 12°, U_{\infty} = 10\ m/s}$, and $\boldsymbol{\sigma = 1.4}$
- Thread configuration: $\boldsymbol{d_t = 7\ \mathrm{mm}}$ and $\boldsymbol{L_t = 1.5\ C_0}$
- A complex interaction is observed

Whipping motion

Rotationa l motion

Analysis of the Whipping Motion

- A Lamb-Oseen vortex profile is considered:

$$v_\theta(r) = \frac{\Gamma}{2\pi r}\left(1 - e^{-1.256(r/r_c)^2}\right) \qquad \text{and} \qquad \frac{\partial p}{\partial r} = \rho\,\frac{v_\theta^2}{r}$$

- Calculating the **attraction force (F_r)** in one-way coupling for various thread diameters and eccentricities results in:

$$F_r = 2r_t \int_0^{\pi} p(\gamma)\cos(\gamma)\,d\gamma$$

- The radial force increases with the thread diameter, **however**, this increase becomes more significant as the thread gets closer and closer to the vortex axis.

- Away from the vortex axis, the relation is almost linear.

- Close to the axis → $\boldsymbol{F_r \propto d_t^2}$

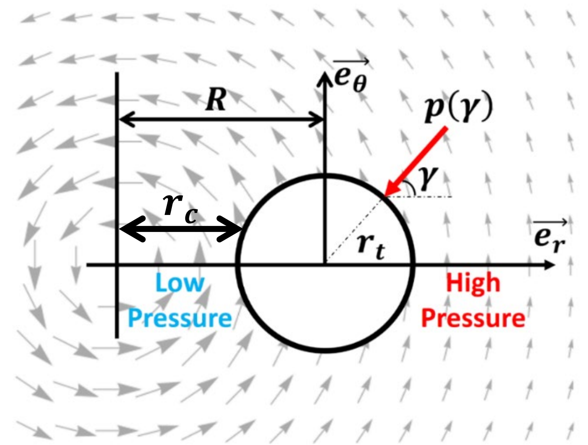

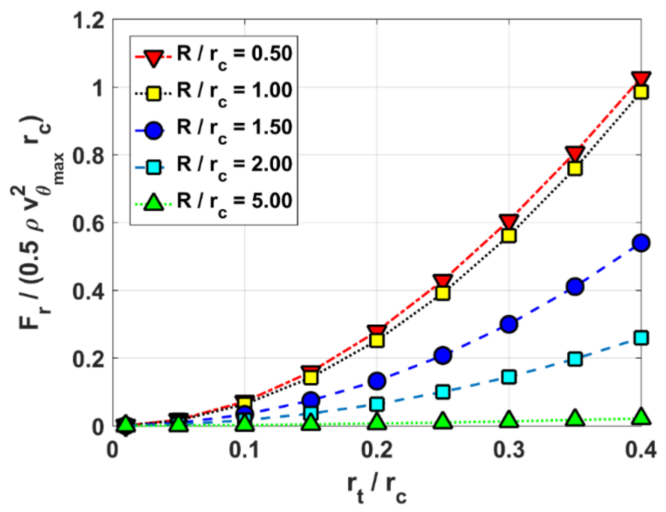

Analysis of the Whipping Motion

Modeling of the coincidence phase:

- The coincidence phase is **fast**, which implies that the **integral parameters** of the vortex should remain constant. ($\Gamma_1 = \Gamma_2 = \Gamma$)

- To find the **new** viscous core radius, we implement the conservation of angular momentum principle:

$$H_1 = \rho L \Gamma \int_0^{\infty} r\left(1 - e^{-1.256(r/r_c)^2}\right) dr$$

$$H_2 = \rho L \Gamma \int_0^{\infty} \frac{r^2}{r - r_t}\left(1 - e^{-1.256\left((r-r_t)/r_{c,2}\right)^2}\right) dr$$

- The coincidence of the thread results in a considerable rise in the minimum pressure induced by the vortex.

- The pressure rise is almost proportional to $\boldsymbol{r_t^{0.2}}$

Arbitrary Lamb-Oseen vortex with $r_c = 1.5$ mm

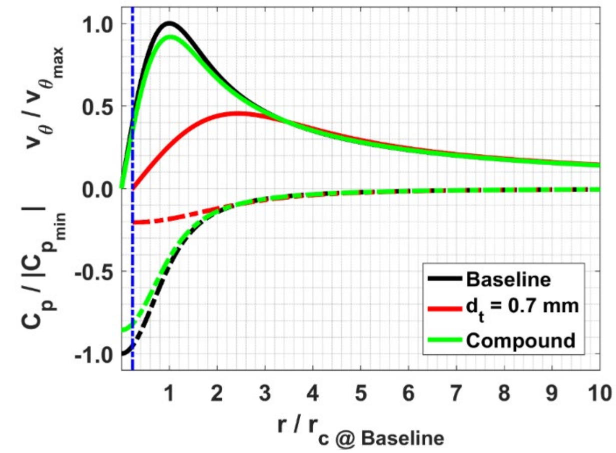

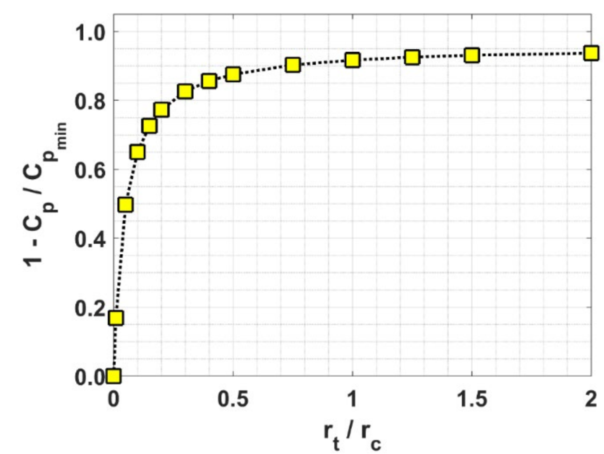

Stereo-PIV setup

- Double-pulsed laser (135 mJ/pulse)
- Seeding particles
  - Hollow glass spheres
  - Average diameter of 10 µm
- 1000 image-pairs for each flow condition
- Vector-to-vector resolution of 0.3×0.4 mm
- Wandering motion correction
  - Center detection by Graftieaux algorithm
  - 2D cubic spline interpolation
- Vatistas vortex model curve-fit

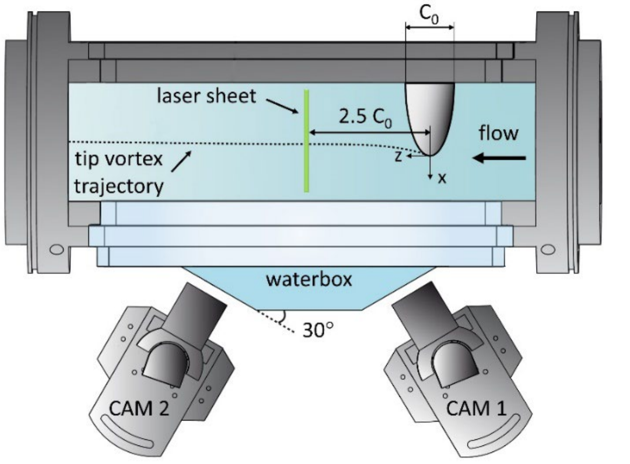

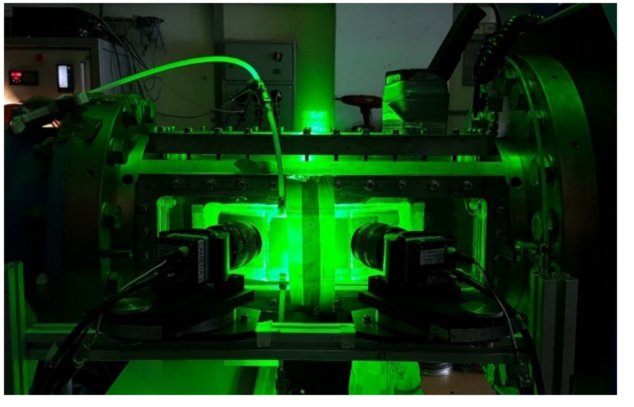

Velocity measurements

Contours of the **tangential** velocity:

- Flow conditions: $\boldsymbol{U_\infty = 10\ \mathrm{m/s}, \alpha = 12°}$
- Thread configuration: $\boldsymbol{d_t = 0.7\ \mathrm{mm}}$
- A clear **reduction** is observed in the magnitude of the tangential velocity.

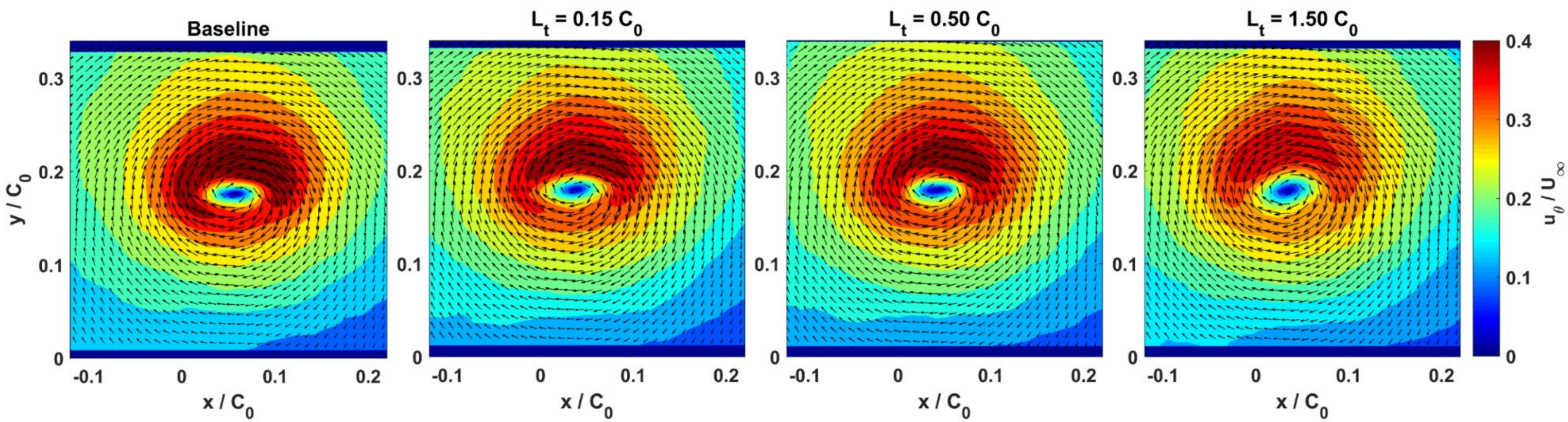

Azimuthally-averaged v_θ profiles

- Test conditions: $\boldsymbol{\alpha = 12°}$, $\boldsymbol{U_\infty = 10\ m/s}$ and $\boldsymbol{d_t = 0.7\ \mathrm{mm}}$.
- A clear **reduction** is observed in the magnitude of the tangential velocity.
- In this test, $L_t = 0.5\ C_0$ is in **non-flapping** state.
  - ➢ The ***winglet effect*** for the rigid structures implies the **augmented turbulent mixing**.

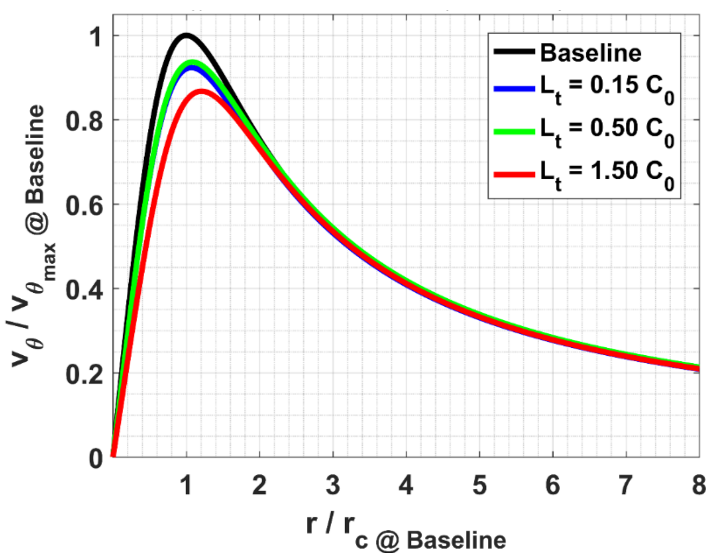

Velocity measurements

Effect of *incidence angle* on tip vortex parameters at various thread lengths.

- Flow conditions: $\boldsymbol{U_\infty = 10\ m/s}$ and non-cavitating regime
- Vortex intensity is conserved and TVC suppression is due to a **viscous core thickening**.

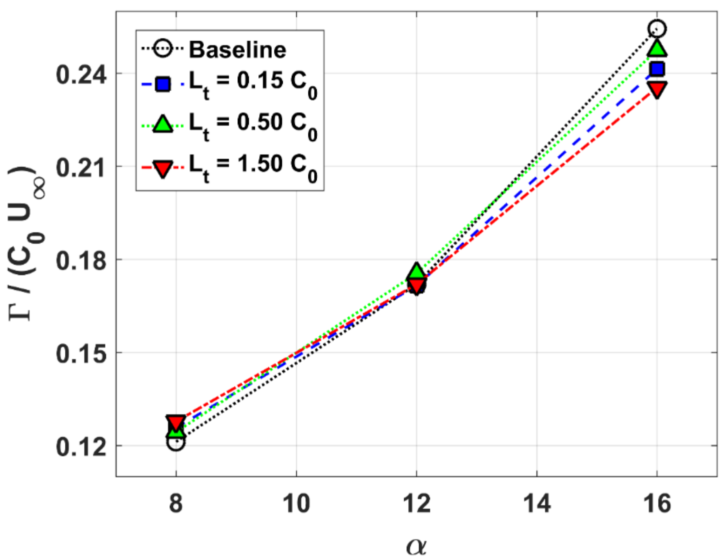

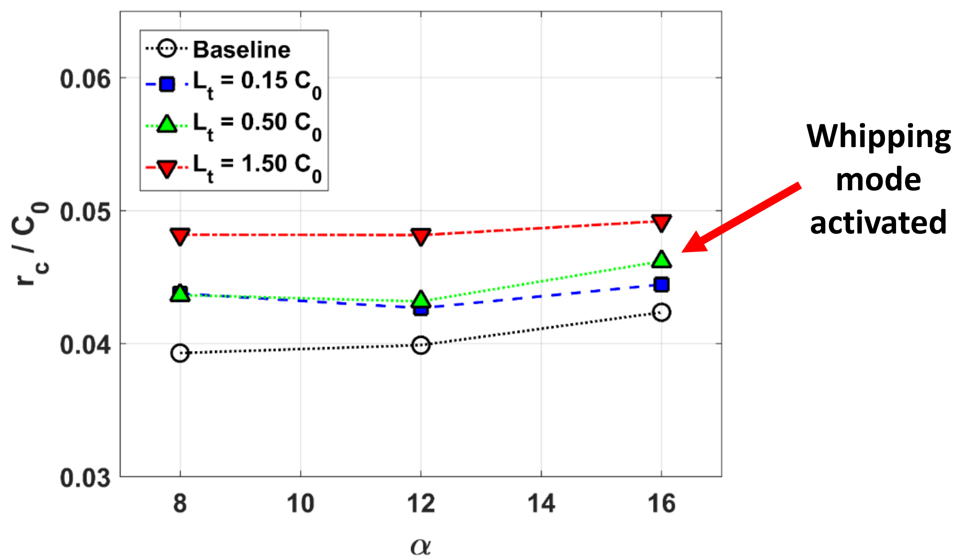

Discussion:

Now, let's put all the **effective parameters** together:

- The extent of thread-vortex interaction → $\boldsymbol{u = \left(\frac{\rho A}{EI}\right)^{1/2} U_\infty L_t}$
- The likelihood of whipping motion → $\boldsymbol{F_r \propto d_t^2}$
- The pressure rise due to the whipping → $\boldsymbol{\Delta p \propto d_t^{0.2}}$

➢ **If we multiply the three terms together and scale the thread diameter with the viscous core radius, we get the following non-dimensional variable:**

$$\boldsymbol{L^* = \frac{4}{r_c^{2.2}} \sqrt{\frac{\rho}{E}} U_\infty L_t d_t^{1.2}}$$

Discussion:

Plotting TVC suppression against the non-dimensional variable:

- The suppression effect is saturated beyond $\boldsymbol{L^* \cong 2}$ for all the configurations.

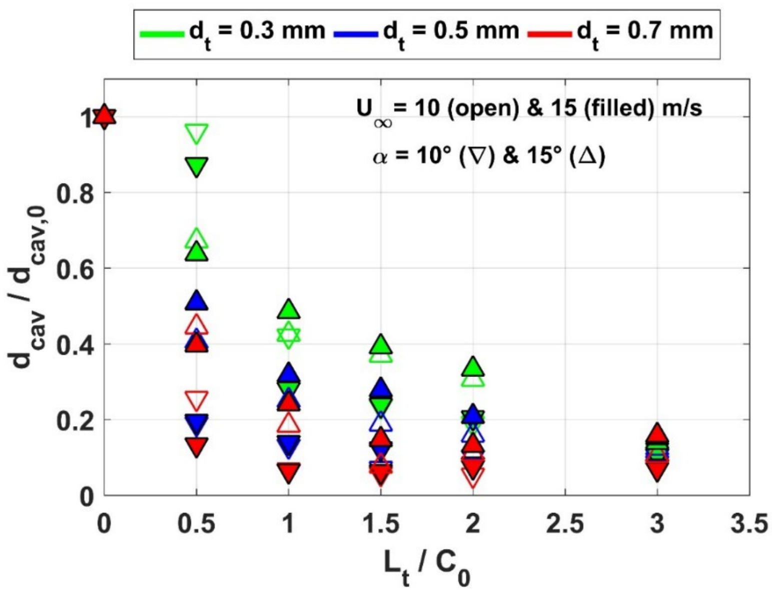

$$K = \frac{4}{r_c^{2.2}}\sqrt{\frac{\rho}{E}}$$

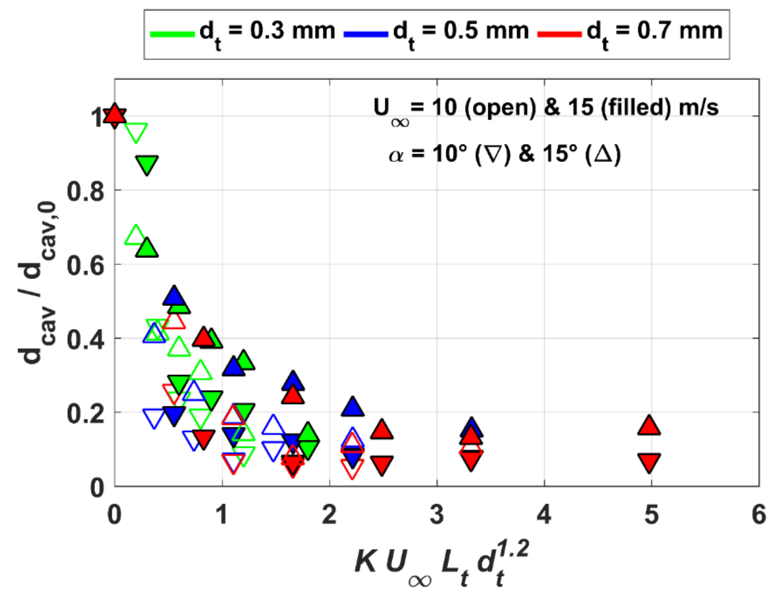

Conclusion

Effectiveness of a flexible thread in TVC mitigation

- A thread should be **flexible enough** to:
  - Get ***aligned*** with the vortex
  - Interact with it ***dynamically***

- **Two interaction/mitigation** regimes:
  - ***Rotational*** motion
  - ***Whipping*** motion

- **Viscous core thickening**